Synthetic Strategy, Magnetic and Spectroscopic Properties of the Terpyridine Complexes $[Cu(terpy)X(H_2O)_n]Y$ (X = NCO, NCS or N_3; n = 0 or 1; Y = NO_3 or PF_6). Crystal Structures of the Azidenitrate and Azidehexafluorophosphate†

Roberto Cortés,[a] M. Karmele Urtiaga,[b] Luis Lezama,[a] Jose Ignacio R. Larramendi,[a] M. Isabel Arriortua[b] and Teófilo Rojo*[,a]

[a] *Departamentos de Química Inorgánica, Universidad de Pais Vasco, Aptdo. 644, 48080-Bilbao, Spain*

[b] *Departamentos de Mineralogía-Petrologia, Universidad del Pais Vasco, Aptdo. 644, 48080-Bilbao, Spain*

Eight copper(II) complexes with 2,2′:6′,2″-terpyridine (terpy) and pseudohalide ligands, $[Cu(terpy)X(H_2O)_n]Y$ [X = NCO, NCS or N_3; n = 0 or 1; Y = NO_3 or PF_6] have been prepared by following a described synthetic strategy. The crystal structures $[Cu(terpy)(N_3)(H_2O)]_x[NO_3]_x$ and $[Cu(terpy)(N_3)(H_2O)]_2[PF_6]_2$ have been determined: monoclinic, space group $P2_1/n$, a = 8.849(2), b = 10.343(1), c = 18.168(3) Å, β = 97.71(2)°, Z = 4; triclinic, space group $P\bar{1}$, a = 9.0609(6), b = 10.2798(8), c = 11.309(1) Å, α = 105.22(7), β = 86.58(7), γ = 112.90(6)°, Z = 2. In both complexes $[Cu(terpy)(N_3)(H_2O)]^+$ entities are present. For the first compound these form a chain structure, *via* hydrogen bonding between the co-ordinated water molecule and the nitrate ion. However, the structure of the second compound is built from dimeric $[Cu_2(terpy)_2(N_3)_2(H_2O)_2]^{2+}$ cations in which the copper ions are connected by one-end bridging azide groups and PF_6^- counter ions. The co-ordination geometry of the copper(II) ion is square pyramidal and octahedral for the two compounds respectively. The complexes studied can be grouped into three structural types, within each of which the compounds are isostructural. The anhydrous and hydrated hexafluorophosphates have dimeric structures; however, the nitrate compounds are associated in chains. Magnetic susceptibility measurements revealed weak magnetic interactions for all of them. The EPR spectra show 'half-field' forbidden transitions for all the complexes and even singlet-to-triplet forbidden transitions for the nitrates. From the positions of these last signals the exchange parameters for the nitrate compounds have been determined. The magnetic interactions have been analysed taking into account several exchange pathways.

The pseudohalides (NCO, NCS, N_3) are known to co-ordinate to metals in different ways, including as terminal or bridging ligands. In the latter category they can act in one-end or end-to-end modes, the former being very scarce. The variety of co-ordination geometries results in a wide range of magnetic behaviours.[1–4]

The most fascinating aspect of the chemistry of the pseudohalide-bridged copper(II) dinuclear complexes is the variety of their magnetic properties. In dibridged complexes with two end-on azido bridges the Cu–N bridging distances are short, see **a**, and the interaction between the metal ions is strongly ferromagnetic.[5,6] In complexes with two end-to-end bridges, and also short Cu–N distances (**b**), the interaction is strongly antiferromagnetic.[7,8] Finally, in complexes with asymmetric end-to-end pseudohalide bridges with both short and long Cu–N bonds (**c**) the interaction is negligible when the geometry around the copper(II) ion is square pyramidal, or very weakly antiferromagnetic when the geometry tends to trigonal bipyramidal.[5,9] An interesting question is, then, what happens in compounds with asymmetric end-on pseudohalide bridges with both short and long Cu–N bonds. Another peculiarity of the di (end-on)pseudohalide bridging mode is that it allows accidental orthogonality, as has been shown experimentally and discussed theoretically.[10–12]

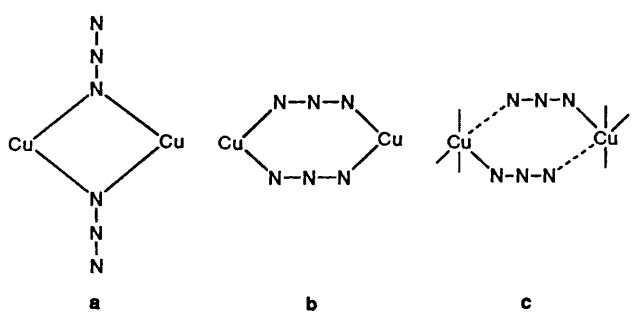

Interesting relationships between rather subtle changes in molecular structure and the net electron exchange have been detected.[13,14] In general a close dependence between the isotropic exchange parameter J and some structural factors has been demonstrated and understood on the basis of the orbital mechanism of the exchange interaction. Spectroscopic techniques, such as EPR, have been shown to be very useful as complements to magnetochemical measurements in copper(II) systems showing weak magnetic interactions.[2,15] This is because they offer more direct access to the singlet–triplet energy gap. The range of exchange energies detectable by EPR spectroscopy is restricted by the microwave radiation used ($2|J| < 0.3$ cm^{-1} for X band).

The synthetic routes for the mono complexes of 2,2′:6′,2″-terpyridine (terpy) include one fundamental way to obtain one-

† *Supplementary data available:* see Instructions for Authors, *J. Chem. Soc., Dalton Trans.*, 1993, Issue 1. pp. xxiii–xxviii.

Non-SI units employed: emu = $10^6/4\pi$ SI, G = 10^{-4} T.

dimensional systems with bivalent metals,[16-18] based on reaction (1) (X = halide or pseudohalide). This method involves

$$[M(terpy)X_2] + Y^-(excess) \longrightarrow [M(terpy)X]Y + X^- \quad (1)$$

the substitution of one ligand by a counter ion, giving the intermediate $[M(terpy)X]^+$, the stacking of which through the X^- anions gives rise to polynuclear compounds (dimers or chains). Owing to the poor effective overlap between the magnetic orbitals determined by this geometry, very low J values (1–3 cm^{-1}) have been observed.[16-19]

In this work, we develop the synthetic strategy to obtain one-dimensional copper(II) systems, with the pseudohalide ligands NCO, NCS and N_3. We report the spectroscopic and magnetic properties of a family of complexes of formula $[Cu(terpy)X(H_2O)_n]Y$ (X = NCO, NCS or N_3; n = 0 or 1; Y = NO_3 or PF_6). The extremely weak exchange interactions of the nitrate complexes have allowed the observation of singlet-to-triplet transitions in the EPR spectra. Crystal structures of the compounds $[Cu(terpy)(N_3)(H_2O)]Y$ (Y = NO_3 or PF_6) are also reported.

Synthetic Strategy.—We previously described a synthetic strategy to obtain one-dimensional copper(II) systems (dimers or chains) formulated [CuL(X)]Y (L = tridentate ligand, X = halide or pseudohalide) starting from $[CuLX_2]$ monomeric compounds.[18] An alternative way of obtaining this type of system has been developed by using as starting material the $[CuL(H_2O)(NO_3)_2]$ complex [easily obtained by reaction of copper(II) nitrate and the tridentate ligand] following Scheme 1.

In all these reactions the $[CuL(X)(H_2O)_n]^+$ entities which are stabilized by planar tridentate ligands are present in solution. The possibility of their stacking through the X^- bridging anions gives rise to polynuclear systems. All compounds containing nitrate as counter ion have shown chain structures.[20] This fact can be explained by the possibility of semi-co-ordination of the nitrate anion, which implies that the $[CuL(X)(H_2O)_n]^+$ units can be extended in space-forming chains. On the other hand, the use of non-co-ordinating counter ions, such as hexafluorophosphate, results in dimeric structures.[20,21]

Experimental

Syntheses of the Compounds.—Copper(II) nitrate trihydrate, potassium hexafluorophosphate, 2,2′:6′,2″-terpyridine, sodium azide, potassium cyanate, and potassium thiocyanate were Merck analytical grade reagents, and used as received.

$[Cu(terpy)X]_2[PF_6]_2$ (X = NCO **1**, NCS **2** or N_3 **3**). To aqueous–methanolic solutions (50 cm^3) of dicyanate, dithiocyanate or diazido complexes $[Cu(terpy)X_2]$ (10^{-3} mol), previously prepared,[22] were added saturated aqueous solutions of potassium hexafluorophosphate. The immediate blue precipitates of compounds **1**–**3** obtained were filtered off, washed with water, and dried under vacuum. Elemental analysis and atomic absorption results are in accord with the formulas $C_{16}H_{11}CuF_6N_4OP$ **1**, $C_{16}H_{11}CuF_6N_4PS$ **2** and $C_{15}H_{11}CuF_6N_6P$ **3** (see Table 1).

$[Cu(terpy)X(H_2O)]_n[NO_3]_n$ (X = NCO **4**, NCS **5** *or* N_3 **6**). Green solutions of compounds **4**–**6** were obtained by adding dropwise (with stirring) aqueous solutions (10 cm^3) containing 10^{-3} mol of potassium cyanate, thiocyanate and sodium azide respectively to previously prepared solutions containing copper(II) nitrate trihydrate (0.241 g, 10^{-3} mol) and 2,2′:6′,2″-terpyridine (0.233 g, 10^{-3} mol). Slow evaporation yielded prismatic crystals. Elemental analysis and atomic absorption results are in accord with the formulas $C_{16}H_{13}CuN_5O_5$, $C_{16}H_{13}CuN_5O_4S$ and $C_{15}H_{13}CuN_7O_4$ respectively (see Table 1).

$[Cu(terpy)X(H_2O)]_2[PF_6]_2$ (X = NCO **7** *or* N_3 **8**). Addition of an excess of saturated aqueous potassium hexafluorophosphate solution to warm aqueous solutions containing complexes **4** and **6** (10^{-3} mol) gave samples of **7** and **8**. The resulting green precipitates were filtered off and readily recrystallized from saturated aqueous solutions. Elemental analysis and atomic absorption results are in accord with the formulas $C_{16}H_{13}CuF_6N_4O_2P$ **7** and $C_{15}H_{13}CuF_6N_6OP$ **8** (see Table 1). All attempts to obtain the thiocyanate complex gave a mixture of products.

Single-crystal and X-Ray Powder Diffraction Data.—Preliminary cell dimensions for compounds **3**, **4** and **6**–**8** were calculated by means of oscillation and Weissenberg photographs obtained for single crystals on a Weissenberg STOE 1971 camera. Powder diffraction patterns for all the eight compounds were obtained on a Philips PW 1470 diffractometer, in the range 2θ 3–60° by using graphite-monochromated Cu-Kα radiation. The powder patterns of compounds **1** and **2** were indexed with the lattice constants of **3** by using the LSUCRE program.[23a] In the same way, the powder pattern of compound **5** can be indexed with the cell parameters of **6**. Analysis of the lattice parameters showed that the eight complexes can be classified in three groups (**I**, **II** and **III**), those within each category being isostructural. Table 2 shows the characterizing parameters for each kind of compound.

Crystal data collection and refinement. Crystals of $[Cu(terpy)(N_3)(H_2O)]NO_3$ **6** and $[Cu(terpy)(N_3)(H_2O)]PF_6$ **8** as green prisms were sealed in glass capillaries before data collection. X-Ray diffraction experiments were performed on an Enraf-Nonius CAD4 automatic diffractometer using graphite-monochromated Mo-Kα radiation (λ = 0.710 69 Å). Crystallographic data, and some features of the data collection and refinements, are listed in Table 3. The unit-cell parameters and orientation matrix were derived from the setting angles of 25 well centred reflections. The observed systematic extinctions for compound **6** were consistent with the space group $P2_1/n$; no systematic extinctions were observed for **8**. Examination of three standard reflections monitored every hour showed no significant intensity decay. Data were corrected for Lorentz and polarization effects, but not for absorption. Initial structures were obtained from isostructural analogous compounds,[20] and refined by full-matrix least-squares techniques (SHELX 76).[23b] All atoms except those of hydrogen were refined anisotropically. The hydrogen positions could be derived from a Fourier difference map. The final difference map showed no significant peaks. The scattering factors were taken from ref. 24. The weighting schemes were of the form $w = 1/[\sigma^2(F) + pF^2]$ where p = 0.000 42 for **6** and 0.001 02 for **8**. The final agreement factors were R = 0.034 (R' = 0.037) for compound **6** and R = 0.044 (R' = 0.045) for **8**. The final positional parameters of the compounds are listed in Tables 4 and 5, respectively.

Additional material available from the Cambridge Crystallo-

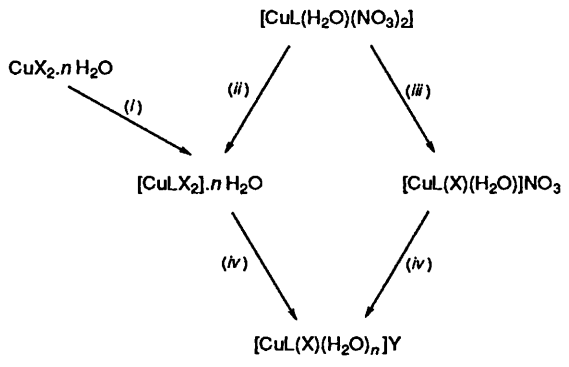

Scheme 1 L = tridentate ligand; X = Cl, Br, NCS, NCO, N_3 or NO_2; Y = PF_6, BF_4 or BPh_4. (*i*) L; (*ii*) excess of X (pseudohalide); (*iii*) 1:1 ratio of X(pseudohalide); (*iv*) excess of Y

Table 1 Elemental analyses and IR data

Compound	Analysis (%)[a] C	H	N	Cu	IR[b]/cm^{-1} ν_{asym}	ν_{sym}	δ
1 [Cu(terpy)(NCO)]PF_6	39.5 (39.7)	2.4 (2.3)	11.2 (11.6)	12.8 (13.1)	2235	1395	640, 615
2 [Cu(terpy)(NCS)]PF_6	38.1 (38.4)	2.1 (2.2)	10.9 (11.2)	12.5 (12.7)	2095	795	470
3 [Cu(terpy)(N_3)]PF_6	36.9 (37.2)	2.1 (2.3)	17.2 (17.4)	12.9 (13.1)	2050	1300	620
4 [Cu(terpy)(NCO)(H_2O)]NO_3	45.3 (45.9)	2.9 (3.1)	16.3 (16.7)	15.3 (15.2)	2225	*c*	615
5 [Cu(terpy)(NCS)(H_2O)]NO_3	44.1 (44.2)	3.2 (3.0)	16.4 (16.1)	14.3 (14.6)	2070	790	475
6 [Cu(terpy)(N_3)(H_2O)]NO_3	43.2 (43.0)	3.0 (3.1)	23.2 (23.4)	14.8 (15.2)	2020	1295	615
7 [Cu(terpy)(NCO)(H_2O)]PF_6	38.6 (38.3)	2.6 (2.7)	11.4 (11.2)	12.5 (12.7)	2230	1390	640, 615
8 [Cu(terpy)(N_3)(H_2O)]PF_6	35.6 (35.9)	2.8 (2.6)	16.5 (16.8)	12.9 (12.7)	2050	1300	620

[a] Calculated values in parentheses. [b] For pseudohalide. [c] Obscured.

Table 2 Representative unit-cell parameters of the complexes [Cu(terpy)X(H_2O)$_n$]Y (X = NCO, NCS or N_3; n = 0 or 1; Y = NO_3 or PF_6) obtained by powder diffraction

	I [Cu(terpy)X]PF_6*	**II** [Cu(terpy)(H_2O)X]NO_3*	**III** [Cu(terpy)(H_2O)X]PF_6*
Symmetry	Monoclinic	Monoclinic	Triclinic
Space group	$P2_1/n$	$P2_1/n$	$P\bar{1}$
a/Å	10.149(2)	8.863(2)	9.059(2)
b/Å	15.593(2)	10.385(2)	10.256(4)
c/Å	11.694(4)	18.169(3)	11.304(4)
α/°			105.12(3)
β/°	103.57(2)	97.62(2)	86.59(2)
γ/°			112.97(3)
U/Å^3	1799(9)	1657.6(4)	932.5(4)
Z	4	4	2
D_m/g cm^{-3}	1.79(2)	1.65(2)	1.75(3)
D_c/g cm^{-3}	1.79	1.68	1.78

* The selected representative parameters correspond to the azide complexes. All have known crystal structures.

Table 3 Data collection and structure refinement for the compounds [Cu(terpy)(N_3)(H_2O)]Y (Y = NO_3 or PF_6)

Formula	$C_{15}H_{13}CuN_7O_4$	$C_{15}H_{13}CuF_6N_6OP$
M	418.84	501.84
System	Monoclinic	Triclinic
Space group	$P2_1/n$	$P\bar{1}$
a/Å	8.849(2)	9.0609(6)
b/Å	10.343(1)	10.2798(8)
c/Å	18.168(3)	11.309(1)
α/°		105.22(7)
β/°	97.71(2)	86.58(7)
γ/°		112.90(6)
U/A^3	1648(3)	935(3)
Z	4	2
D_m/g cm^{-3}	1.65(2)	1.75(3)
D_c/g cm^{-3}	1.68	1.78
μ(Mo-Kα)/cm^{-1}	13.6	13.3
F(000)	844	498
Scan type	ω–2θ	ω–2θ
θ Range/°	1–27	1–25
Check reflections	21 – 9, 2 – 5 – 3, 3 – 51	253, 254, – 12 – 3
No. measured reflections	3579	5896
h, k, l Interval	± 11, 13, 23	12, ± 14, ± 15
No. variables	284	311
No. unique reflections [$I \geqslant 2.5\sigma(I)$]	2044	2078

graphic Data Centre comprises H-atom coordinates, thermal parameters and remaining bond lengths and angles.

Other Measurements.—Infrared spectra were obtained using a Perkin-Elmer 1430 spectrophotometer, with KBr pellets, in the 4000–250 cm^{-1} region. Magnetic measurements were carried out in the temperature range 4.2–100 K using a DSM8 susceptometer-magnetometer. Experimental susceptibilities were corrected for the diamagnetic contributions and for the temperature-independent paramagnetism, estimated to be 60 × 10^{-6} cm^3 mol^{-1} per copper(II) ion. The EPR spectra were recorded on powdered samples at X-band frequency with a Bruker E.S.P. 300 spectrometer, equipped with a standard Oxford low-temperature device, calibrated by an NMR probe for the magnetic field. The frequency was measured by using a Hewlett–Packard 5352B microwave frequency counter.

Results and Discussion

Structures of [Cu(terpy)(N_3)(H_2O)]Y (Y = NO_3 **6** *or* PF_6 **8**).—Tables 6 and 7 show the main interatomic distances and angles of compounds **6** and **8** respectively. Table 7 also includes data for the anhydrous hexafluorophosphate compound **3** to facilitate comparison with the hydrated one **8**. For compounds **6** and **8**, the crystal structures consist of [Cu(terpy)(N_3)(H_2O)]$^+$ cations and Y$^-$ anions (Y = NO_3 or PF_6). Fig. 1 shows an

Table 4 Fractional atomic coordinates ($\times 10^4$) for $[Cu(terpy)(N_3)(H_2O)]NO_3$

Atom	*x*	*y*	*z*
Cu	1078.3(5)	4258.7(4)	4191.6(2)
N(1)	6(4)	5602(3)	3481(2)
N(2)	2028(3)	5842(3)	4599(2)
N(3)	2383(4)	3544(3)	5114(2)
N(4)	−403(4)	2934(4)	3911(2)
N(5)	−331(4)	1793(4)	3972(2)
N(6)	−363(5)	685(4)	4024(2)
N(7)	6963(4)	−564(4)	6830(2)
O(1)	6668(4)	573(3)	6961(2)
O(2)	6500(4)	−1060(3)	6226(2)
O(3)	7739(4)	−1188(4)	7315(2)
O(w)	2764(4)	3766(3)	3435(2)
C(1)	−991(5)	5350(5)	2873(2)
C(2)	−1543(5)	6302(6)	2387(3)
C(3)	−1043(6)	7544(5)	2510(2)
C(4)	−20(5)	7826(4)	3125(2)
C(5)	492(4)	6827(4)	3596(2)
C(6)	1654(4)	6971(4)	4261(2)
C(7)	2344(5)	8104(4)	4528(2)
C(8)	3472(5)	8042(4)	5139(2)
C(9)	3860(5)	6863(4)	5474(2)
C(10)	3098(4)	5769(4)	5197(2)
C(11)	3295(4)	4447(4)	5492(2)
C(12)	4321(5)	4117(4)	6112(2)
C(13)	4424(5)	2855(4)	6344(2)
C(14)	3501(6)	1951(5)	5956(2)
C(15)	2493(5)	2313(4)	5353(2)

Table 5 Fractional atomic coordinates ($\times 10^4$) for $[Cu(terpy)(N_3)(H_2O)]PF_6$

Atom	*x*	*y*	*z*
Cu	6 557.2(8)	843.2(6)	9 057.6(6)
N(1)	7 806(5)	2 724(4)	10 341(4)
N(2)	6 050(5)	2 231(4)	8 460(4)
N(3)	5 127(5)	−513(4)	7 573(4)
N(4)	6 427(6)	−629(5)	9 866(5)
N(5)	7 396(6)	−1 033(4)	10 112(4)
N(6)	8 261(7)	−1 502(7)	10 375(6)
O(w)	8 929(5)	1 003(4)	8 083(4)
C(1)	8 736(7)	2 896(6)	11 288(5)
C(2)	9 528(7)	4 227(7)	12 109(5)
C(3)	9 353(8)	5 440(7)	11 947(5)
C(4)	8 407(7)	5 286(6)	10 962(5)
C(5)	7 661(6)	3 928(5)	10 177(4)
C(6)	6 635(6)	3 640(5)	9 092(4)
C(7)	6 258(7)	4 635(6)	8 698(6)
C(8)	5 231(8)	4 139(7)	7 678(6)
C(9)	4 614(7)	2 682(7)	7 066(6)
C(10)	5 036(6)	1 726(6)	7 470(5)
C(11)	4 504(6)	123(6)	6 943(5)
C(12)	3 482(7)	−643(7)	5 940(6)
C(13)	3 077(8)	−2 136(8)	5 509(7)
C(14)	3 737(8)	−2 767(8)	6 126(7)
C(15)	4 727(7)	−1 963(6)	7 148(6)
P	8 506(2)	−2 612(2)	5 571(2)
F(1)	9 184(5)	−3 860(4)	5 351(4)
F(2)	9 648(7)	−1 959(5)	4 578(4)
F(3)	7 814(4)	−1 361(3)	5 762(3)
F(4)	9 875(5)	−1 601(5)	6 576(4)
F(5)	7 463(6)	−3 191(6)	6 605(5)
F(6)	7 153(6)	−3 614(4)	4 578(5)

ORTEP[25] drawing of the cation which stacks to give a chain structure for the nitrate and a dimer for the hexafluorophosphate.

$[Cu(terpy)(N_3)(H_2O)]_x[NO_3]_x$ **6**. The cationic complex units $[Cu(terpy)(N_3)(H_2O)]^+$ (Fig. 1) are linked by hydrogen bonds between the water molecules and the nitrate anions to give a linear chain structure [H(w2)···O(2^{III}) 2.13(5); H(w1)···O(1^{IV}) 2.07(5) Å; III $1-x, -y, 1-z$; IV $-\frac{1}{2}+x, \frac{1}{2}-y, -\frac{1}{2}+z$] as shown in Fig. 2. The structure is propagated through a helicoidal binary axis along the |010| direction. The intrachain Cu···Cu^{I} distance is 7.3267(6) Å (I $1-x, 1-y, 1-z$), while the Cu···Cu^{II} interchain distance is 4.0140(6) Å (II $-x, 1-y, 1-z$). As Fig. 1 illustrates, the co-ordination around the copper(II) ions can be described as distorted square pyramidal, with the terpy ligand [Cu–N(1), N(2), N(3) 2.041(3), 1.941(3), 2.041(3) Å] and the nitrogen atom of the azide group [Cu–N(4) 1.917(4) Å] in the basal positions, while the water molecule [Cu–O(w) 2.220(2) Å] occupies the apical position. The *trans*-basal angles N(1)–Cu–N(3) and N(2)–Cu–N(4) are 158.3(1) and 161.8(1)°, respectively. The distortions of the co-ordination polyhedron from the square pyramid (*SPY*) to the trigonal bipyramid (*TBPY*), calculated by the Muetterties and Guggenberger models,[26] give a value $\Delta = 0.75$, close to that of square-pyramidal geometry. The basal atoms are coplanar within the range ± 0.04 Å, the copper(II) ion being 0.18 Å out of this mean plane.

The interatomic bond distances and angles for the terpyridine ligand are similar to those found in other related com-

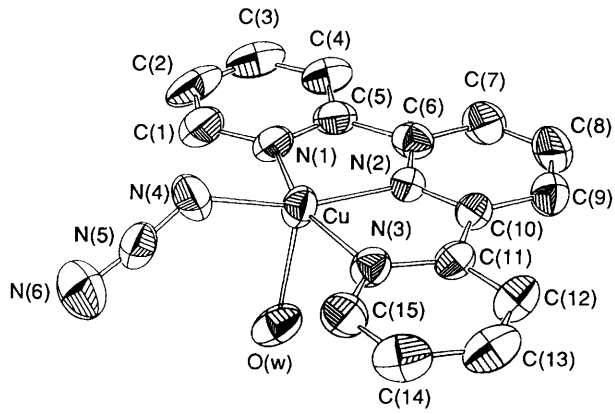

Fig. 1 An ORTEP drawing of the cationic complex $[Cu(terpy)(N_3)(H_2O)]^+$ showing the atom numbering

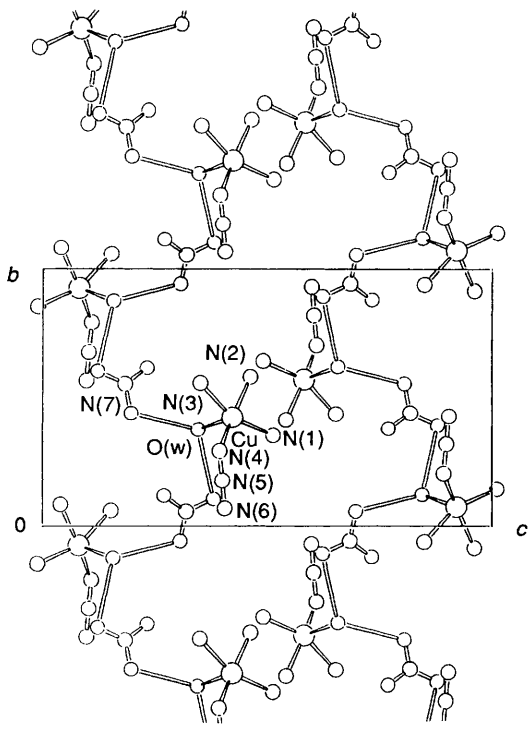

Fig. 2 Perspective view of the chaining of the $[Cu(terpy)(N_3)(H_2O)]NO_3$ complexes in the |010| direction

Table 6 Selected bond distances (Å) and angles (°) for [Cu(terpy)-$(N_3)(H_2O)]NO_3$

Copper(II) co-ordination sphere			
Cu–N(1)	2.041(3)	Cu–N(2)	1.941(3)
Cu–N(3)	2.041(3)	Cu–N(4)	1.917(4)
Cu–O(w)	2.220(2)	Cu · · · Cu^{I}	7.3267(6)
Cu · · · Cu^{II}	4.0140(6)		
N(1)–Cu–N(2)	78.9(1)	N(1)–Cu–N(3)	159.3(1)
N(1)–Cu–N(4)	94.3(1)	N(1)–Cu–O(w)	93.4(1)
N(2)–Cu–N(3)	79.9(1)	N(2)–Cu–N(4)	161.8(1)
N(2)–Cu–O(w)	79.9(1)	N(3)–Cu–N(4)	104.5(1)
N(3)–Cu–O(w)	94.1(1)	N(4)–Cu–O(w)	99.4(1)
O(w)–Cu–$O(2^{III})$	103.8(1)	O(w)–Cu–$O(1^{IV})$	111.1(1)
Average values in the terpy ligand			
C–N	1.341(2)	C–C(intraring)	1.375(2)
C–C(interring)	1.466(3)	C–H	0.97(2)
C–C–C(intraring)	121.1(3)	C–C–C(interring)	125.3(2)
C–C–N(intraring)	122.3(2)	C–C–N(interring)	114.5(1)
C–N–C	119.8(2)		
Azide ligand			
N(4)–N(5)	1.186(6)	N(5)–N(6)	1.151(6)
Cu–N(4)–N(5)	131.3(3)	N(4)–N(5)–N(6)	175.5(4)
Nitrate ion			
N(7)–O(1)	1.234(5)	N(7)–O(2)	1.231(5)
N(7)–O(3)	1.226(5)		
O(1)–N(7)–O(3)	118.4(4)	O(2)–N(7)–O(3)	120.6(4)
O(1)–N(7)–O(2)	121.0(4)		

I $1-x, 1-y, 1-z$; II $-x, 1-y, 1-z$; III $1-x, -y, 1-z$; IV $-\frac{1}{2}+x, \frac{1}{2}-y, \frac{1}{2}+z$.

pounds.[16,17] The angles N(2)–Cu–N(1) and N(2)–Cu–N(3) deviate from 90° by about 10° and the Cu–N(2) bond distance is shorter than the corresponding distances to N(1) and N(3) by about 0.1 Å, its rigidity being once again confirmed.

The copper(II) ion forms an angle with the azide group [Cu–N(4)–N(5)] of 131.3(3)°. A highly planar configuration is observed for the nitrate ion, the largest deviation from the N(7),O(1),O(2),O(3) mean plane being 0.004 Å for the N(7) atom. The values of the N–O bond distances and O–N–O bond angles (1.220 Å and 120°, respectively) show a good agreement with those in the literature.[14,27]

$[Cu(terpy)(N_3)(H_2O)]_2[PF_6]_2$ **8**. In this crystal structure copper-containing cations $[Cu(terpy)(N_3)(H_2O)]^+$ pair up to result in centrosymmetric one-end azide-bridged dimers. A drawing of the dimeric molecule is shown in Fig. 3. The geometry about the copper atom can be described as essentially a distorted octahedron. In the case of the anhydrous compound this geometry is reduced to an elongated square pyramid. The three nitrogens of the terpy ligand are in the equatorial plane [Cu–N(1), N(2), N(3) 2.036(3), 1.933(5), 2.016(4) Å] together with the nitrogen atom of one azide bridge [Cu–N(4) 1.927(6) Å]. The nitrogen atom of the second azide bridging group [Cu–$N(4^{I})$ 2.851(5) Å (I $1-x, -y, 2-z$)] and a water molecule [Cu–O(w) 2.323(5) Å] occupy the axial positions. The axial distance is significantly shorter in the anhydrous complex, Cu–$N(4^{I})$ 2.469(6) Å. The four co-ordinating atoms in the equatorial plane are essentially coplanar. The copper(II) ion is displaced 0.17 Å from this mean plane. The closest approach of two dimers is 7.643(1) Å for Cu · · · Cu^{II} (II $2-x, -y, 2-z$) in compound **8**, being slightly different from that observed in the anhydrous complex [Cu · · · Cu^{II} 7.369(2) Å].

The azide ions in both complexes **3** and **8** bridge between two copper centres through one nitrogen atom (end-on bridging mode). Each bridging N atom simultaneously occupies an equatorial position on Cu and an axial position on Cu^{I}. The

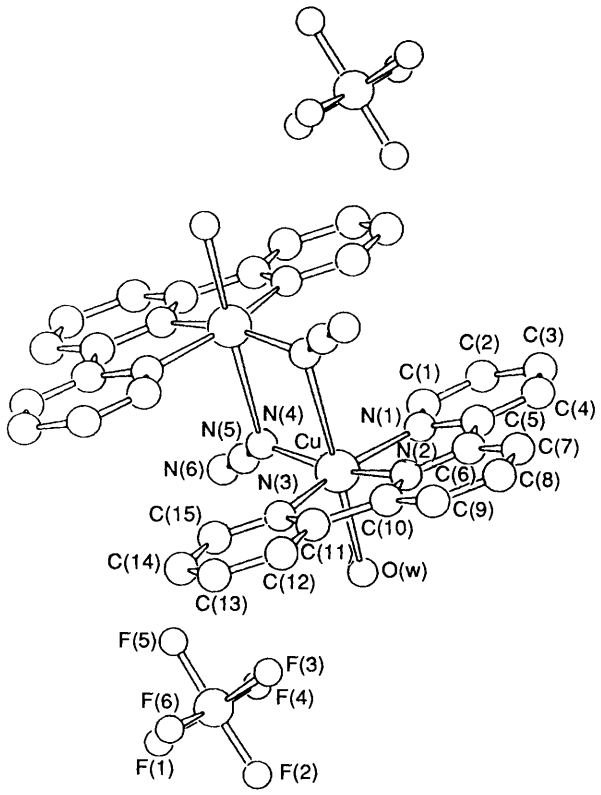

Fig. 3 Perspective view of the dimeric compound $[Cu(terpy)(N_3)-(H_2O)]_2[PF_6]_2$

axial distance is larger than the corresponding equatorial one. In the bridging unit, the intradimeric Cu · · · Cu^{I} distances are 3.595(1) and 3.313(2) Å for **8** and **3**, respectively. The bridging angles Cu–N(4)–Cu^{I} are 95.7(2) (**8**) and 96.3(3)° (**3**).

As in the azidenitrate complex, the interatomic bond distances and angles corresponding to the terpy ligand are similar to those found in other related compounds,[16,17] confirming the planarity and rigidity of this ligand.

The values of the P–F bond distances in the hexafluorophosphate group and the high isotropic thermal parameters of its fluorine atoms are similar to those found in other related PF_6^- containing terpyridine complexes.[4,16,17]

Infrared Spectroscopy.—The infrared spectra of the compounds have been analysed, in particular the bands due to the water molecules, pseudohalide ligands (see Table 1) and counter ions. In the 3500–3250 cm^{-1} regions two bands appear, corresponding to the stretching vibration of the water molecules for compounds **4**–**8**. These bands are shifted to lower frequencies for the nitrate complexes, due to hydrogen bonding. The bending vibrations can be observed at approximately 1640 cm^{-1}.

For the NCO-bridged compounds, the bands corresponding to the antisymmetric stretching vibration of the cyanate ligand, $\nu_{asym}(NCO)$, appear at approximately 2230 cm^{-1} for compounds **1** and **7** and 2225 cm^{-1} for **4**. The $\nu_{sym}(NCO)$ vibration can be observed as weak bands at about 1390 cm^{-1}, except for the nitrate complex for which this band is obscured by one corresponding to the nitrate group. The δ(NCO) vibration can be used to predict the existence of NCO bridging groups, because a splitting is observed in this case. This vibration mode is split in two bands (640, 615 cm^{-1}) for the hexafluorophosphate complexes **1** and **7**, in good agreement with the existence of end-on bridging NCO groups.

For the thiocyanate complexes the ν(CN) band corresponding to the NCS group occurs at 2095 cm^{-1} for the dimer **2**. This value (below 2100 cm^{-1}) argues strongly in favour of the

Table 7 Selected bond distances (Å) and angles (°) for $[Cu(terpy)(N_3)(H_2O)_n]PF_6$ (n = 0 or 1)

	n = 0	n = 1		n = 0	n = 1
Copper co-ordination sphere					
Cu–N(1)	2.030(8)	2.036(3)	Cu–N(2)	1.933(6)	1.933(5)
Cu–N(3)	2.005(7)	2.016(4)	Cu–N(4)	1.954(7)	1.927(6)
Cu–N(4^{I})	2.269(6)	2.851(5)	Cu–O(w)		2.323(5)
Cu · · · Cu^{II}	7.369(2)	7.643(1)	Cu · · · Cu^{I}	3.313(2)	3.595(1)
O(w)–Cu–N(1)		89.2(2)	O(w)–Cu–N(2)		100.0(2)
O(w)–Cu–N(3)		94.6(2)	O(w)–Cu–N(4)		97.6(2)
N(1)–Cu–N(2)	80.1(3)	80.0(2)	N(2)–Cu–N(3)	80.1(3)	79.8(2)
N(3)–Cu–N(4)	104.4(3)	97.2(2)	N(1)–Cu–N(4)	95.9(3)	102.0(2)
N(1)–Cu–N(3)	158.5(3)	159.8(2)	N(2)–Cu–N(4)	173.8(3)	163.3(2)
N(4^{I})–Cu–N(1)	92.2(2)	94.5(2)	N(4^{I})–Cu–N(2)	91.7(2)	69.8(2)
N(4^{I})–Cu–N(3)	96.8(2)	75.9(2)	N(4^{I})–Cu–N(4)	83.7(2)	84.3(2)
O(w)–Cu–N(4^{I})	165.1(2)	165.1(2)	Cu–N(4)–Cu^{I}	96.3(3)	95.7(2)
Average values in the terpy ligand					
C–N	1.34(2)	1.34(2)	C–C(intraring)	1.39(4)	1.38(2)
C–C(interring)	1.48(1)	1.48(1)	C–H	0.9(1)	0.9(1)
C–C–C(intraring)	119(1)	119(1)	C–C–C(interring)	124(1)	124(1)
C–C–N(intraring)	121(1)	121(1)	C–C–N(interring)	112.6(8)	112.6(9)
C–N–C	120(2)	119(2)			
Azide ligand					
N(4)–N(5)	1.20(1)	1.181(9)	N(5)–N(6)	1.15(9)	1.154(10)
Cu–N(4)–N(5)	129.4(5)	132.4(5)	N(4)–N(5)–N(6)	174.5(8)	175.5(8)
Hexaflurophosphate anion					
P–F(1)	1.572(9)	1.586(5)	P–F(2)	1.44(2)	1.581(5)
P–F(3)	1.48(1)	1.599(4)	P–F(4)	1.54(2)	1.573(5)
P–F(5)	1.48(1)	1.551(7)	P–F(6)	1.49(2)	1.549(5)

I 1 − x, −y, 2 − z; II 2 − x, −y, 2 − z.

Table 8 Structural, EPR and magnetic parameters for the present and related complexes

Compound	$g_{\|\|}$		$g_{\perp}$	Other signals	Cu–X_{bridge} (Å)	Bridge angle (°)	Geometry[a]	J/cm^{-1}	Ref.
1	2.24		2.04	ΔM_s = 2				+1.4	This work
2	2.26		2.05	ΔM_s = 2				—	This work
3	—		—	ΔM_s = 2	2.469(6) 1.954(7)	96.3(3)	*SPY*	—	21, this work
4	—		—	ΔM_s = 2[b]			*SPY*	|0.12|	20
5	2.25	2.11	2.03	ΔM_s = 2[b]			*SPY*	|0.12|	This work
6	2.26		2.10	ΔM_s = 2[b]			*SPY*	|0.14|	This work
7	2.21		2.07	ΔM_s = 2	3.368(7) 1.906(8)	83.5(3)	*OC*	< −0.5	20
8	2.25		2.10	ΔM_s = 2	2.851(5) 1.927(6)	95.7(2)	*OC*	−2.9	This work
9[a]		2.15			2.043(2) 1.990(2)	105.46(9) 101.65(8)	*OC*	+70 ± 20	5
10[a]	2.21	2.06	2.00	—	1.99(1) 1.97(1)	100.5	*SP*	+105 ± 20	29
11[e]		2.17		—	2.015(1) 1.915(1)	95.7(1) 102.5	*SP*	> +200	6

[a] *SPY* = Square pyramidal, *OC* = octahedral, *SP* = square planar. [b] Singlet–triplet. [c] $[Cu_2(N_3)_4L(H_2O)]$ (L = 1,4,7,13,16,19-hexaoxa-10,22-diazacyclotetracoscane). [d] $[Cu_2(4Bu^t\text{-py})(N_3)_2][ClO_4]_2$ (4Bu^t-py = 4-*tert*-butylpyridine). [e] $[Cu_2(tmen)_2(N_3)(OH)][ClO_4]_2$ (tmen = *N*,*N*,*N*′,*N*′-tetramethylethylenediamine).

presence of 'end-on' N(CS) bridging groups,[28] in good agreement with the crystallographic results. Besides, only one band corresponding to the ν(CS) vibration can be observed at 795 cm^{-1}, and the δ(NCS) bending mode appears at 470 cm^{-1}. The bands observed for the thiocyanatenitrate complex **5** [ν(CN) at 2070, ν(CS) at 790 and δ(NCS) at 475 cm^{-1}] are in good accord with a terminal NCS group.

The bands corresponding to the $\nu_{asym}(N_3)$ stretching vibrations can be observed at 2050 cm^{-1} for the anhydrous and hydrated azide hexafluorophosphate complexes **3** and **8**, in good agreement with the existence of 'end-on' bridging azide groups. The azide symmetric stretch, $\nu_{sym}(N_3)$, is observed at about 1300 cm^{-1} in both cases, and the signal at 620 cm^{-1} corresponds to the bending vibration (δ). For the azidenitrate complex **6** the $\nu_{asym}(N_3)$ stretching vibration appears at lower energy (2020 cm^{-1}), corresponding to the existence of one terminal azide group, in good accord with the structural results.

The active bands corresponding to the hexafluorophosphate ion appear approximately at 840 (ν_3) and 540 cm^{-1} (ν_4) for all the compounds studied. They are not split, indicating that these

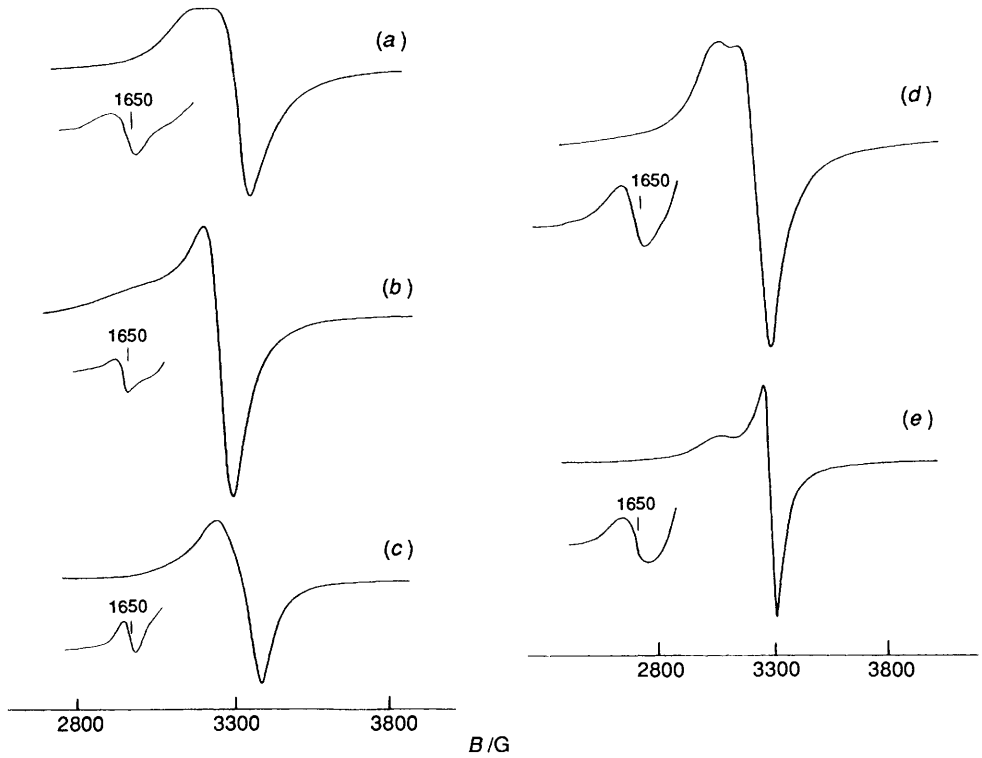

Fig. 4 X-Band EPR spectra, at 4.2 K, of $[Cu(terpy)X]_2[PF_6]_2$ [X = NCO (*a*), NCS (*b*) or N_3 (*c*)] and $[Cu(terpy)X(H_2O)]_2[PF_6]_2$ [X = NCO (*d*) or N_3 (*e*)]

groups act only as counter ions. The bands corresponding to the nitrate ion appear at 1340 cm^{-1} in all cases, with a splitting which is indicative of the semico-ordination of these groups to give the chain structure.

Electron Paramagnetic Resonance.—X-Band EPR spectra have been recorded for powdered samples of all eight copper(II) compounds, at 4.2 K. Fig. 4 shows the observed spectra for **1–3**, **7** and **8**, and Fig. 5 the corresponding spectra of **4–6**. Table 8 gives the EPR parameters obtained for these and other related complexes.

The EPR spectra of the anhydrous hexafluorophosphate compounds **1–3** show an axial symmetry for the g tensor, with $g_{\|}$ values near 2.25 and $g_{\perp}$ close to 2.05, in accord with square-pyramidal copper(II) geometries. Besides these large signals, which correspond to the $\Delta M_s = \pm 1$ allowed transitions, the three complexes exhibit the 'half-field' $\Delta M_s = \pm 2$ forbidden transition, indicative of a magnetic coupling between two copper(II) ions.

The spectrum of the thiocyanatenitrate compound **5** shows a rhombic symmetry for the g tensor in the $\Delta M_s = \pm 1$ region, with $g_1 = 2.25, g_2 = 2.11, g_3 = 2.03$. A 'half-field' signal is seen at 1650 G corresponding to the $\Delta M_s = \pm 2$ transition. The spectrum of the azidenitrate complex **6** shows an axial signal with $g_{\|} = 2.26$ and $g_{\perp} = 2.10$ for the $\Delta M_s = \pm 1$ transition. The $\Delta M_s = \pm 2$ transition is also observed. Furthermore, two very weak signals, symmetrically located at lower (720 G) and higher (5600 G) field than the normal $\Delta M_s = \pm 1$ transitions are observed for both compounds. These signals can be assigned as the forbidden singlet–triplet transitions. Each of these transitions is separated from the allowed one by a field value of $2|J|(g\beta)^{-1}$. With the average g values equal to 2.12, the calculated exchange parameters are $|J| = 0.12$ and 0.14 cm^{-1} for compounds **5** and **6** respectively, in good accord with the magnetic susceptibility measurements. Similar results were obtained for the cyanatenitrate compound.[20]

The EPR spectra of compounds **7** and **8** show an axial symmetry for the g tensor with $g_{\|} = 2.21$ and $g_{\perp} = 2.07$ and $g_{\|} = 2.25$ and $g_{\perp} = 2.10$, respectively, corresponding to the $\Delta M_s = \pm 1$ transition. The $\Delta M_s = \pm 2$ transition is observed at approximately 1650 G, indicating magnetic interactions between copper(II) pairs.

Magnetic Behaviour.—Magnetic susceptibility measurements have been performed within the temperature range 4.2–150 K. Fig. 6(*a*) shows the thermal variation of the reciprocal susceptibility, together a plot of $\chi_m T$ *vs.* T, for the compounds **1–3**. The corresponding measurements on compounds **7** and **8** are illustrated in Fig. 6(*b*).

Magnetic measurements of the hexafluorophosphate compounds **1–3** show a Curie–Weiss behaviour in the range 10–150 K, the Weiss temperatures θ being +0.9, +0.3 and −0.5 K for compounds **1**, **2** and **3** respectively. The Curie constants are approximately 0.42 cm^3 K mol^{-1} in all cases. The $\chi_m T$ products are practically temperature-independent for $T > 10$ K, reaching values of 0.52 (NCO), 0.44 (NCS) and 0.33 (N_3) cm^3 K mol^{-1} when cooling from this temperature to 4.2 K. These variations may be indicative of weak ferromagnetic interactions for compounds **1** and **2**, and indicate antiferromagnetism for **3**. In all cases the $|J|$ values are lower than 1 cm^{-1}. The weakness of the magnetic couplings for **2** and **3** makes us unable to determine the exchange parameter J. However, for the cyanate dimer **1**, taking into account its proposed crystal structure, the magnetic behaviour may be described by using the Bleaney–Bowers equation for two copper atoms,[30] derived from the Heisenberg isotropic spin Hamiltonian ($H = -2J\hat{S}_1\hat{S}_2$), for two coupled $S = \frac{1}{2}$ ions, equation (2) where

$$\chi = \frac{Ng^2\beta^2}{kT}\left(\frac{2}{3 + \exp(-2J/kT)}\right) + N\alpha \qquad (2)$$

$N\alpha = 60 \times 10^{-6}$ cm^3 mol^{-1} per copper(II) ion. The best least-squares fit [solid line in Fig. 6(*a*)] is obtained with the parameter $J = +1.4$ cm^{-1} and g fixed at 2.11 as obtained from the EPR measurements.

In the case of the nitrate compounds **4–6** a Curie–Weiss law is

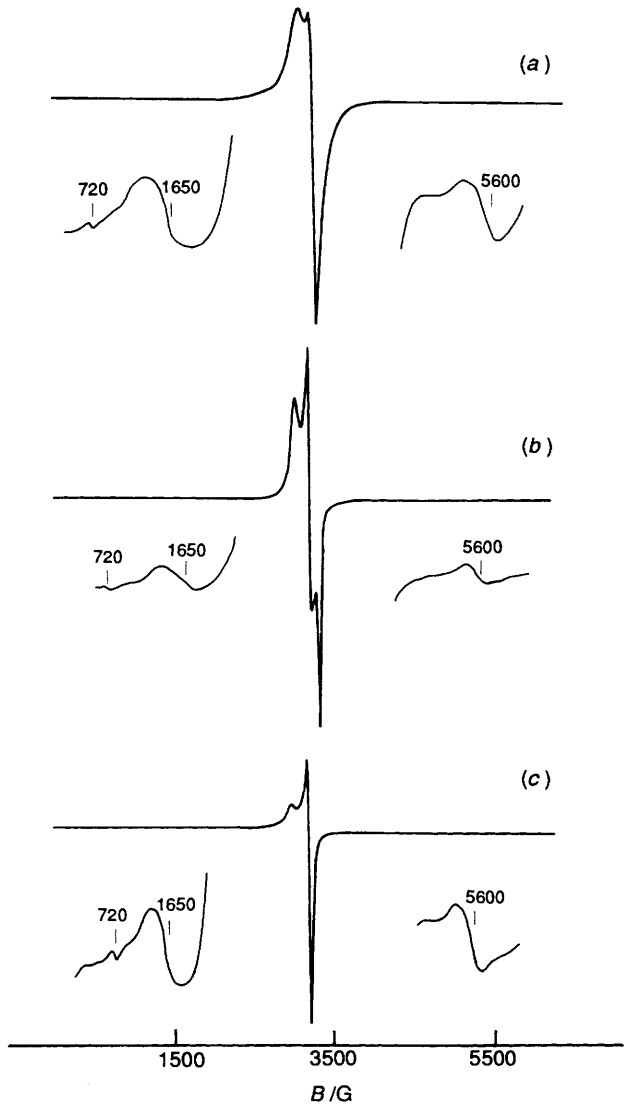

Fig. 5 X-Band EPR spectra at 4.2 K of the complexes [Cu(terpy)X(H_2O)]NO_3 [X = NCO (*a*), NCS (*b*) or N_3 (*c*)]

also followed for $T > 5$ K, with negative intercepts of about −0.5 K in all cases. These negative θ values and the overall appearance of the $\chi_m T$ *versus* T curves [decreasing $\chi_m T$ from 0.42 (150 K) to 0.30 cm^3 K mol^{-1} (4.2 K) for the three compounds] are indicative of very weak antiferromagnetic interactions, in good agreement with the values obtained by EPR measurements [$|J| = 0.12$ (for **4**, **5**) and 0.14 cm^{-1} (for **6**), respectively].

The magnetic susceptibility data, shown in Fig. 6(*b*), for the hydrated hexafluorophosphate compounds are well described by a Curie–Weiss law above 6 K, with θ = −1 K and $C = 0.44$ cm^3 K mol^{-1}, and above 20 K with θ = −2.8 K and $C = 0.42$ cm^3 K mol^{-1}, for compounds **7** and **8**, respectively. The $\chi_m T$ values decrease from 0.44 (150) to 0.29 cm^3 K mol^{-1} (4.2 K) for the cyanate **7**, while for the azide complex **8** $\chi_m T$ ranges, from 0.42 (150) to 0.18 cm^3 K mol^{-1} (4.2 K). These results are indicative of antiferromagnetic interactions in both compounds. The J parameter of **7** could not be determined, due to the weakness of the magnetic coupling. However, least-squares fitting of the susceptibility data by the Bleaney–Bowers[30] equation for the azide dimer **8** gives $J = -2.9$ cm^{-1} with $g = 2.12$ as determined by EPR measurements.

Exchange-interaction Pathways.—First let us consider the pseudohalide-bridged hexafluorophosphate dimers. The interaction between the two metal atoms leads to two molecular states, namely a spin singlet $S = 0$ and a spin triplet $S = 1$, separated by $2J$. The interaction is antiferromagnetic if $S = 0$ is the ground state (J negative), ferromagnetic if $S = 1$ is the ground state (J positive). The singlet–triplet energy gap $2J$ may be expressed in a relatively simple way as the sum of two components,[31] an antiferromagnetic negative component J_{AF} and a positive ferromagnetic component J_F [equation (3)],

$$J = J_{AF} + J_F \quad (3)$$

where $J_{AF} = -2S\Delta$ and $J_F = 2j$; S is the overlap integral between the magnetic orbitals, j the two-electron exchange integral, and Δ the energy gap between the two molecular orbitals in the dimer constructed from the magnetic orbitals, for the $S = 1$ state. Whereas ferromagnetic contributions are usually small, the magnitude of the antiferromagnetic ones is proportional to the square of the overlap integral,[32] $J_{AF} \propto S^2$. The resulting sign of the magnetic interactions will depend then to a great extent on the amplitude of that overlap.

From the structural results it can be seen that the exchange interactions between copper(II) pairs observed in the hexafluorophosphate dimer compounds (**1–3**, **7** and **8**) (see Table 8 and Fig. 7) are propagated through the N-pseudohalide bridging groups. The geometry of the dimeric cations $[Cu_2(terpy)_2X_2]^{2+}$ (X = NCO, NCS or N_3) which are present in these compounds is unfavourable to transmit the exchange coupling. In a copper(II) environment which is an ideal regular square pyramid the J constant would be zero due to the fact that the $x^2 - y^2$ magnetic orbitals are essentially localized in the basal planes.[33] The distortion towards trigonal-bipyramidal or octahedral co-ordination exhibited for the copper(II) polyhedra in the reported dimers permits the magnetic orbitals to acquire some z^2-type character. The resulting delocalization on the apical site (z direction) allows a weak interaction to occur. The magnetic couplings can then be explained in terms of the topology of the bridges between the copper atoms. Within each group of dimers the change in bridging ligands is reflected in the different strengths of the magnetic interactions, increasing in the order NCS < NCO < N_3. This is indicative of a greater interaction of the exchange-propagating orbitals of the azide ligand, lying at higher energy, with the $d_{x^2-y^2}$ metal orbitals. The difference in the strength of the magnetic interactions for these complexes can be explained by considering Fig. 7. The compound $[Cu(terpy)(NCO)(H_2O)]_2[PF_6]_2$ **7** shows a weaker antiferromagnetic behaviour than does the related azide **8** owing to the larger Cu–N(4^1) distance (3.368 and 2.851 Å respectively). The influence of the bridging angle, taking into account the large distance between the two portions of the cyanate dimer **7**, is less important in this case. The change in the co-ordination polyhedron {octahedral for $[Cu(terpy)(N_3)(H_2O)]_2[PF_6]_2$ and square pyramidal for anhydrous $[Cu(terpy)(N_3)]_2[PF_6]_2$} can explain the stronger antiferromagnetic behaviour observed for the hydrated compound with respect to the anhydrous one, owing to the greater z^2-type character for the octahedral geometry. This geometric change is much more important for the propagation of the magnetic interactions than both the slow variation of the bridging angle and the shortening in Cu–N(4^1) bond distance (compound **3**).

If we compare our hexafluorophosphate dimers with other related complexes reported in the literature (compounds **9–11**) shown in Table 8, it can be seen that the latter show stronger antiferromagnetic interactions. This fact can easily be explained because their magnetic orbitals lie in the same plane together with the bridging atoms of the pseudohalide ligand, which makes possible greater overlap, and as a consequence increases the antiferromagnetic interactions.

On the other hand, the structural arrangement found in the nitrate complexes **4–6** permits the existence of several potential interaction pathways.

(1) Taking into account the relatively short minimum

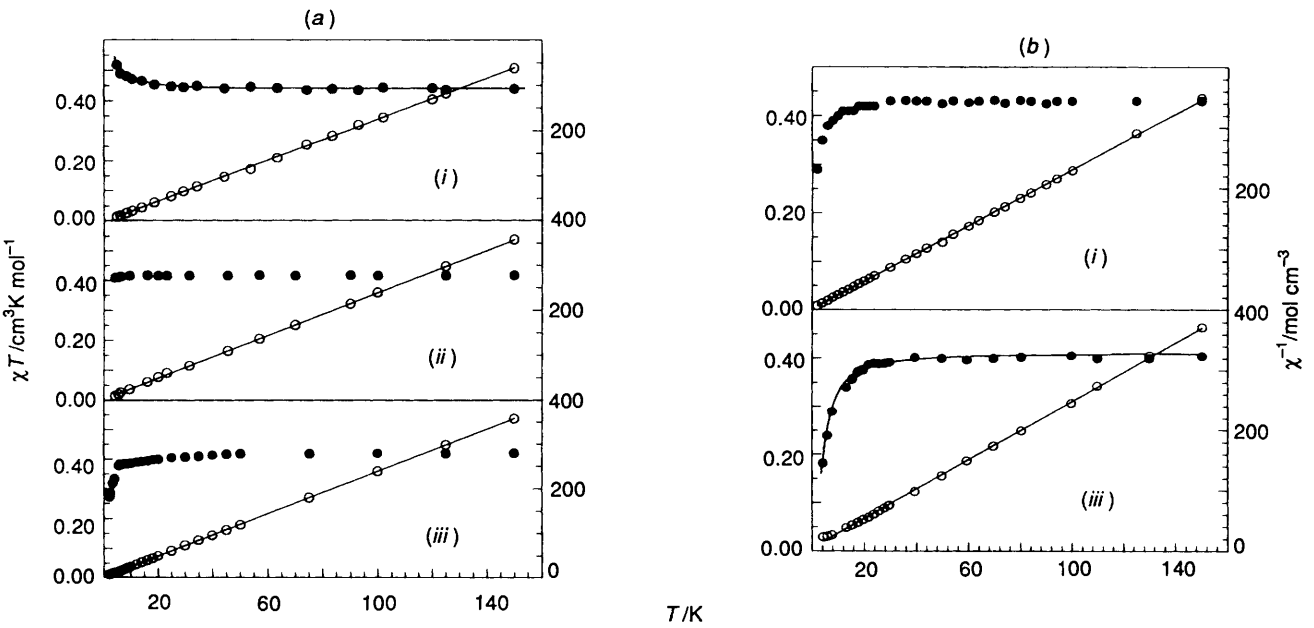

Fig. 6 Thermal variation of the reciprocal susceptibility and of the product χT for the anhydrous (n = 0) (*a*) and hydrated (n = 1) (*b*) pseudohalidehexafluorophosphate dimers $[Cu(terpy)X(H_2O)_n]PF_6$ [X = NCO (*i*), NCS (*ii*) or N_3 (*iii*)]

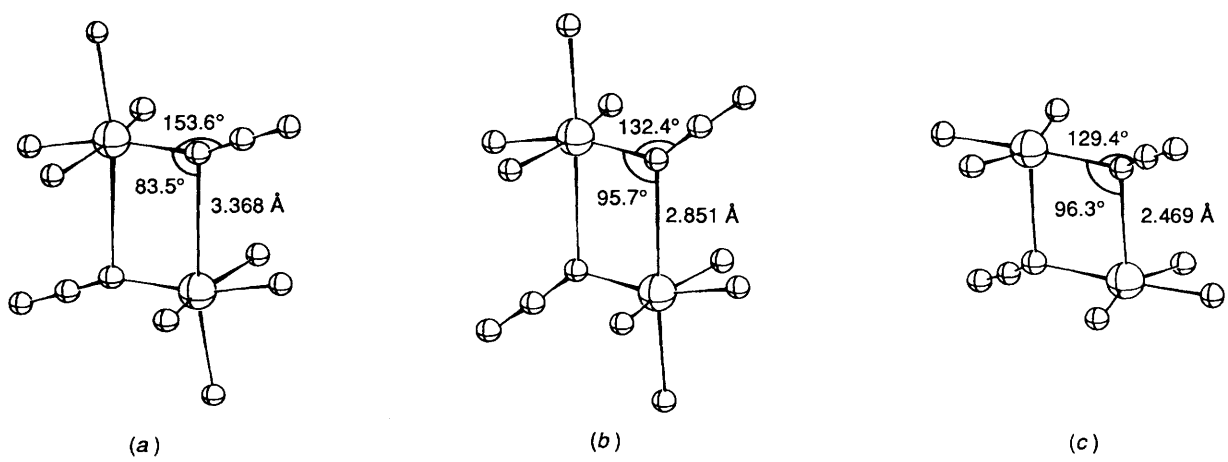

Fig. 7 Comparison of the co-ordination polyhedra for the $[Cu(terpy)(NCO)(H_2O)]_2[PF_6]_2$ (*a*), $[Cu(terpy)(N_3)(H_2O)]_2[PF_6]_2$ (*b*) and $[Cu(terpy)(N_3)]_2[PF_6]_2$ (*c*)

interchain Cu···Cu distances for these nitrate complexes [4.0140(6) Å for the azide compound **6**], the existence of a direct dipolar interaction can be considered. The value of the dipolar parameter calculated for this complex, by using expression (4),

$$D_d = \langle g \rangle^2 \beta^2 / r^3 \quad (4)$$

is D_d = 0.04 cm^{-1}, which *a priori* cannot be neglected in comparison to the J value obtained from the EPR spectrum (0.14 cm^{-1}).

(2) A superexchange 'complex' path can be proposed by considering a very extended bridging network formed by two water molecules and one nitrate anion connected by hydrogen bonds (Fig. 2), with an estimated Cu···Cu intrachain distance of 12.7 Å for complex **6**. This alternative path seems, *a priori*, to be reasonable, given the ability of nitrate and water molecules to support the exchange. According to the experimentally determined function for long-range ferromagnetic and antiferromagnetic superexchange proposed by Coffman and Buettner,[34] which establishes the limit of exchange interactions observed at any distance, the expected J value for such a large exchange distance must be less than 10^{-2}–10^{-3} cm^{-1}. Though the observed $|J|$ value (0.14 cm^{-1}) is higher than that expected it is not conclusive, because several exceptions to these rules have been found.

(3) A close inspection of the structures of these nitrate complexes lets us introduce an alternative superexchange pathway. This involves a 'quasi-direct' interaction through both the pseudohalide groups and the pyridine rings of the terpyridine ligands belonging to two chains related by an inversion centre, chains which are separated by approximately 3.5 Å. This path is shown in Fig. 8. In accord with the results obtained from the magnetic measurements and the EPR spectra, this mechanism seems to be the most reasonable to propagate the exchange in this kind of compound.

Conclusion

For the first time, the proposed synthetic strategy has successfully been employed to obtain copper(II) polynuclear complexes. Polynuclear compounds of three types are formed by $[Cu(terpy)X(H_2O)_n]^+$ cations (X = NCO, NCS or N_3; n = 0 or 1) and Y^- anions (Y = NO_3 or PF_6). These cationic copper(II) complexes stack to give dimeric arrangements in types **I** and **III** (in all cases through one-end pseudohalide bridging networks) which are very scarce. On the other hand, chain

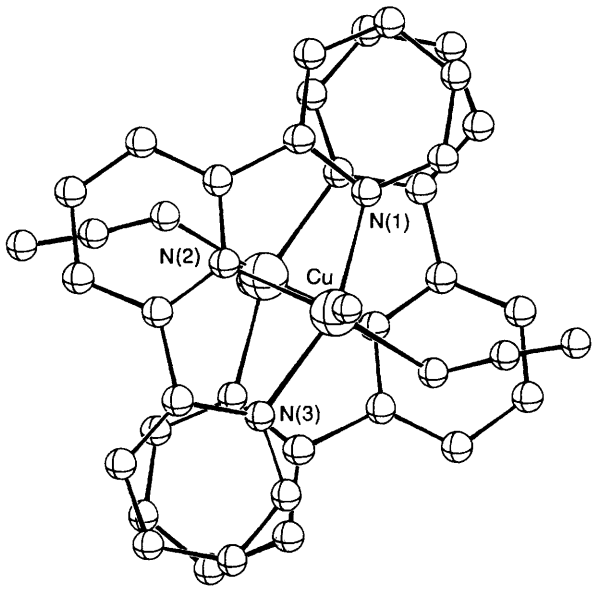

Fig. 8 View of the overlapping between the pyridine rings of the terpy ligands for the $[Cu(terpy)X(H_2O)]NO_3$ complexes

structures are formed in type **II** compounds. The variation of the pseudohalide ligands within each category has no influence on the resulting products, giving the same structural arrangements. However, the counter ion used has a significant influence on the final structural disposition. The chain structures can be explained by the semi-co-ordination possibility that the nitrate ion offers, while the hexafluorophosphate ion does not permit this. The differences between the compounds of types **I** and **III**, which are obtained by two different synthetic methods, are the co-ordinated water molecule and the larger $Cu–N_{axial}$ distance in the latter.

With respect to the magnetic measurements, it can be seen that the anhydrous and hydrated hexafluorophosphate dimers, having asymmetric end-on pseudohalide bridges with short and long Cu–N bridging bonds, show both weak antiferromagnetic and ferromagnetic exchange interactions. The geometry of the bridging units is unfavourable for transmitting the exchange coupling. An increase in the strength of the antiferromagnetic interactions can be observed on going from the square-pyramidal co-ordination polyhedron for the copper(II) ion in the anhydrous dimeric compounds (where the magnetic orbitals are practically of $x^2 - y^2$ type and are sited in parallel planes) to an octahedral disposition in the hydrated ones (where the magnetic orbitals acquire some z^2-type character).

For the nitrate compounds the exchange interactions are very weak, but their magnitude has been estimated from the singlet-to-triplet EPR transitions. The analysis of their potential interaction pathways leads us to conclude that these interactions seem to be transmitted through both the pseudohalide ions and the terpy ligands that are sited on parallel planes at a ≈ 3.5 Å separation, this interaction being of a π–π type.

Acknowledgements

This work was supported by grants from the Direccion General de Investigación Científica y Técnica (DGICYT PB90-0549) and Universidad del Pais Vasco-Euskal Herriko Unibertsitatea (U.P.V. 130.310.E116/91), which we gratefully acknowledge.

References

1 D. M. Duggan and D. N. Hendrickson, *Inorg. Chem.*, 1973, **12**, 2422.
2 D. M. Duggan and D. N. Hendrickson, *Inorg. Chem.*, 1974, **13**, 2929.
3 E. J. Laskowsky, D. M. Duggan and D. N. Hendrickson, *Inorg. Chem.*, 1975, **14**, 2449.
4 M. I. Arriortua, R. Cortés, J. L. Mesa, L. Lezama, T. Rojo and G. Villeneuve, *Transition Met. Chem.*, 1988, **13**, 371.
5 P. Comarmond, P. Plumere, J. M. Lehn, Y. Angus, R. Louis, R. Weiss, O. Kahn and I. Morgenstern-Badarau, *J. Am. Chem. Soc.*, 1982, **104**, 6330.
6 O. Kahn, S. Sikorav, J. Gouteron, S. Jeannin and Y. Jeannin, *Inorg. Chem.*, 1983, **22**, 2877.
7 R. Agnus, R. Louis and R. Weiss, *J. Am. Chem. Soc.*, 1979, **101**, 3381.
8 V. McKee, J. V. Dagdigian and R. Bau, *J. Am. Chem. Soc.*, 1981, **103**, 7000.
9 I. Bkouche-Waksman, S. Sikorav and O. Kahn, *J. Cryst. Spectrosc. Res.*, 1983, **13**, 303.
10 O. Kahn and M. F. Charlot, *Nouv. J. Chim.*, 1980, **4**, 567.
11 P. J. Hay, J. C. Thibeault and R. Hoffmann, *J. Am. Chem. Soc.*, 1975, **97**, 4884.
12 V. M. Crawford, H. W. Richardson, J. R. Wason, D. J. Hodgson and W. E. Hatfield, *Inorg. Chem.*, 1976, **15**, 2107.
13 G. R. Hall, D. M. Duggan and D. N. Hendrickson, *Inorg. Chem.*, 1975, **14**, 1956.
14 O. P. Anderson, A. B. Packard and M. Wicholas, *Inorg. Chem.*, 1976, **15**, 1613.
15 C. G. Pierpont, L. C. Francesconi and D. N. Hendrickson, *Inorg. Chem.*, 1977, **16**, 2367.
16 T. Rojo, M. I. Arriortua, J. Ruiz, J. Darriet, G. Villeneuve and D. Beltrán, *J. Chem. Soc., Dalton Trans.*, 1987, 285.
17 T. Rojo, M. I. Arriortua, J. L. Mesa, R. Cortés, G. Villeneuve and D. Beltrán, *Inorg. Chim. Acta*, 1987, **134**, 59.
18 T. Rojo, J. L. Mesa, M. I. Arriortua, J. M. Savariault, J. Galy, G. Villeneuve and D. Beltrán, *Inorg. Chem.*, 1988, **27**, 3904.
19 J. V. Folgado, E. Coronado and D. Beltrán, *J. Chem. Soc., Dalton Trans.*, 1986, 1061.
20 T. Rojo, R. Cortés, L. Lezama, J. L. Mesa, J. Vía and M. I. Arriortua, *Inorg. Chim. Acta*, 1989, **165**, 91.
21 M. I. Arriortua, K. Urtiaga, M. Insausti, J. L. Mesa and T. Rojo, *Polyhedron*, 1991, **10**, 2451.
22 T. Rojo, A. García, J. L. Mesa, M. I. Arriortua, J. L. Pizarro and A. Fuertes, *Polyhedron*, 1989, **8**, 97; M. I. Arriortua, J. L. Mesa, T. Rojo, T. Debaerdemaeker, D. Beltrán, H. Stratemeier and D. Reinen, *Inorg. Chem.*, 1988, **27**, 2976; J. Via, M. I. Arriortua, T. Rojo, J. L. Mesa and A. García, *Bull. Soc. Chim. Belg.*, 1989, **98**, 179.
23 (*a*) D. E. Appleman and H. T. Evans, LSUCRE, Indexing and Least-squares Refinement of Powder Diffraction Data, Report PB-216188, U.S. Department of Commerce, N.T.I.S., Springfield, VA, 1973; (*b*) G. M. Sheldrick, SHELX 76, Program for Crystal Structure Determination, University of Cambridge, 1976.
24 *International Tables for X-Ray Crystallography*, Kynoch Press, Birmingham, 1974, vol. 4, p. 99.
25 C. K. Johnson, ORTEP, Report ORNL-3794, Oak Ridge National Laboratory, Oak Ridge, TN, 1965.
26 E. L. Muetterties and L. J. Guggenberger, *J. Am. Chem. Soc.*, 1974, **96**, 1748.
27 O. P. Anderson, *Inorg. Chem.*, 1975, **14**, 730.
28 J. L. Mesa, T. Rojo, M. I. Arriortua, G. Villeneuve, J. V. Folgado, A. Beltrán and D. Beltrán, *J. Chem. Soc., Dalton Trans.*, 1989, 53.
29 S. Sikorav, I. Bkouche-Waksman and O. Kahn, *Inorg. Chem.*, 1984, **23**, 490.
30 B. Bleaney and K. D. Bowers, *Proc. R. Soc. London, Ser. A*, 1952, **214**, 451.
31 J. J. Girerd, Y. Journaux and O. Kahn, *Mol. Phys.*, 1977, **34**, 1063.
32 O. Kahn, *Angew. Chem., Int. Ed. Engl.*, 1985, **24**, 834.
33 O. Kahn, I. Morgestern-Badarau and R. Block, *Chem. Phys. Lett.*, 1984, **108**, 457.
34 R. E. Coffman and G. R. Buettner, *J. Chem. Phys.*, 1979, **83**, 2387.

Received 16*th July* 1993; *Paper* 3/04179D